

Electronic Supporting information

for

**More complex than originally thought: revisiting origins of the relaxation
processes in the dimethylammonium zinc formate**

Table S1. Crystal data, data collection and refinement results for partially DMAZnD

Crystal data	
Chemical formula	C ₁₀ H ₁₆ D ₆ N ₂ O ₁₂ Zn ₂
<i>M_r</i>	499.07
Crystal system, space group	Triclinic, <i>P1</i>
Temperature (K)	100
<i>a</i> , <i>b</i> , <i>c</i> (Å)	8.1573 (9), 8.1491 (7), 8.8244 (10)
α, β, γ (°)	61.343 (10), 62.557 (11), 60.057 (10)
<i>V</i> (Å ³)	426.70 (10)
<i>Z</i>	1
<i>m</i> (mm ⁻¹)	2.88
Crystal size (mm)	0.15 × 0.10 × 0.08
Data collection	
No. of measured, independent and observed [<i>I</i> > 2σ(<i>I</i>)] reflections	3141, 3141, 2758
(sin <i>q</i> / <i>l</i>) _{max} (Å ⁻¹)	0.707
Refinement	
<i>R</i> [<i>F</i> ² > 2σ(<i>F</i> ²)], <i>wR</i> (<i>F</i> ²), <i>S</i>	0.052, 0.145, 1.06
No. of reflections	3141
No. of parameters	236
No. of restraints	87
H-atom treatment	H-atom parameters constrained
Dρ _{max} , Dρ _{min} (e Å ⁻³)	1.38, -1.36

Absolute structure	Classical Flack method preferred over Parsons because s.u. lower.
Absolute structure parameter	0.39 (4)

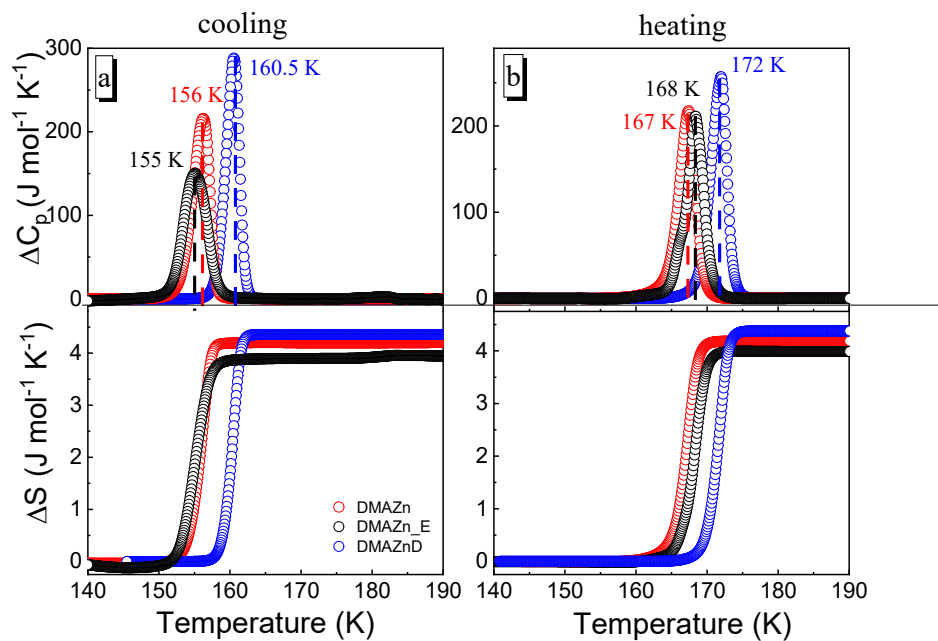


Figure S1 The change in the heat capacity and entropy related to the phase transition in DMAZn^1 , DMAZn_E and DMAZnD^2 measured in (a) cooling and (b) heating modes.

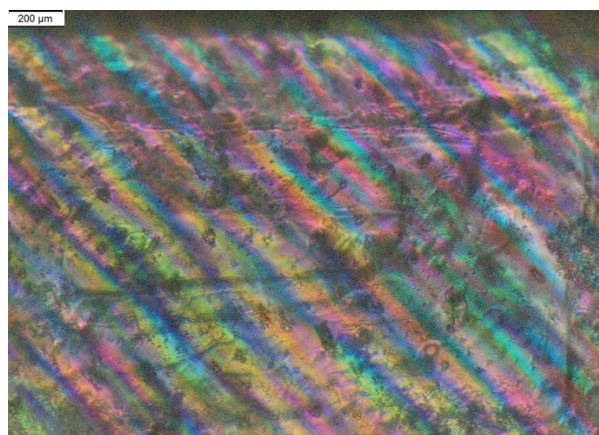


Figure S2 The ferroelastic domain structure of DMAZn .

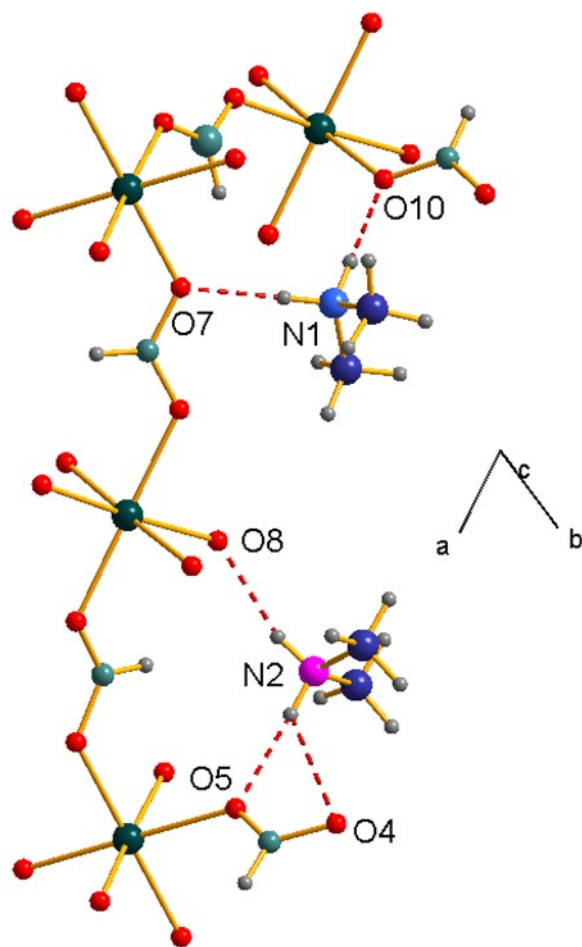


Figure S3 Atom numbering scheme for hydrogen-bonds. DMAZn-formate, $T=100\text{K}$.

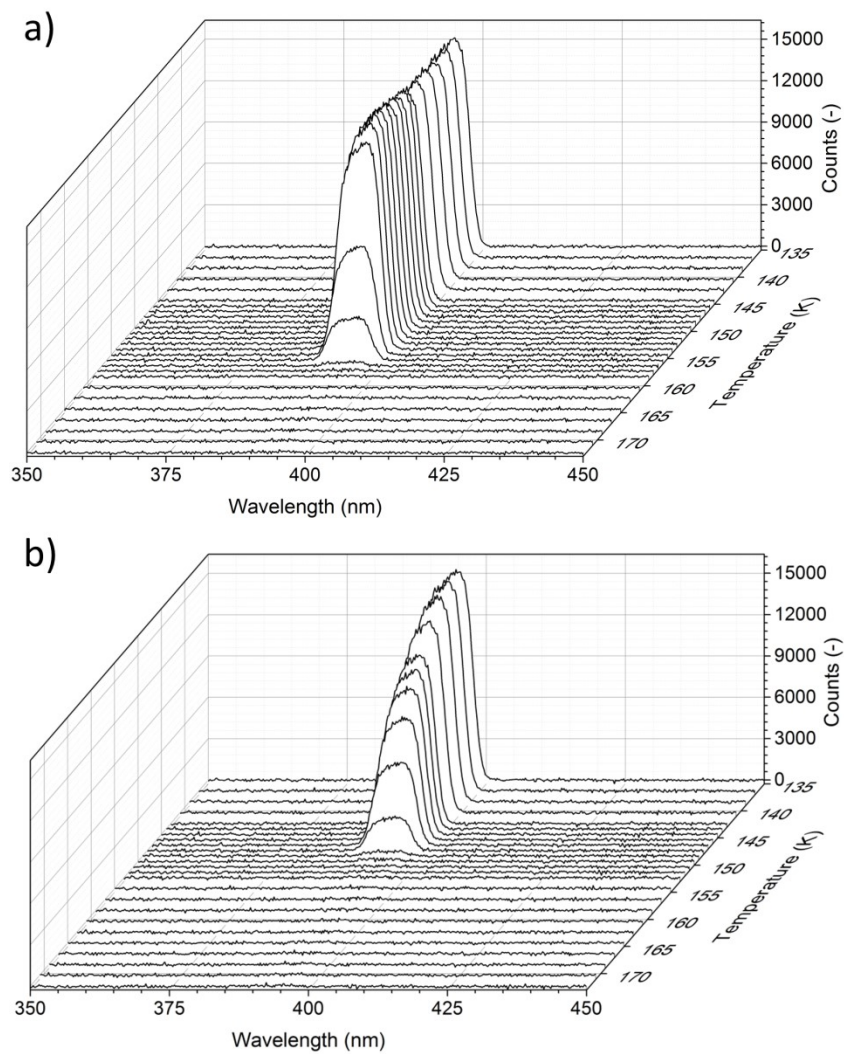


Figure S4. Experimental SHG spectra obtained upon a) heating run and b) cooling run.

Table S2. Selected geometric parameters (\AA , $^\circ$)

Zn1—O3	2.081 (11)	O3—C7	1.229 (17)
Zn1—O4	2.090 (11)	O4—C8	1.289 (13)
Zn1—O9	2.101 (10)	O5—C8 ⁱ	1.238 (17)
Zn1—O8	2.106 (9)	O6—C9 ⁱⁱ	1.243 (14)
Zn1—O2	2.115 (10)	O7—C10 ⁱⁱⁱ	1.258 (14)
Zn1—O10	2.139 (10)	O8—C6	1.278 (15)
Zn2—O6	2.068 (10)	O9—C10	1.256 (16)
Zn2—O11	2.095 (8)	O10—C5	1.250 (15)
Zn2—O12	2.098 (10)	O11—C5 ^{iv}	1.261 (18)
Zn2—O1	2.103 (11)	O12—C6 ^v	1.269 (14)
Zn2—O7	2.107 (11)	C1—N1	1.46 (2)
Zn2—O5	2.136 (10)	C2—N1	1.44 (2)
O1—C7	1.272 (15)	C3—N2	1.51 (2)
O2—C9	1.236 (15)	N2—C4	1.49 (2)
O3—Zn1—O4	94.6 (4)	O6—Zn2—O5	84.7 (4)
O3—Zn1—O9	177.3 (5)	O11—Zn2—O5	179.6 (6)
O4—Zn1—O9	87.7 (4)	O12—Zn2—O5	90.2 (4)
O3—Zn1—O8	93.0 (4)	O1—Zn2—O5	90.9 (5)
O4—Zn1—O8	90.8 (4)	O7—Zn2—O5	88.3 (4)
O9—Zn1—O8	88.3 (4)	C7—O1—Zn2	126.0 (8)
O3—Zn1—O2	90.4 (4)	C9—O2—Zn1	125.7 (9)
O4—Zn1—O2	91.1 (4)	C7—O3—Zn1	125.8 (7)
O9—Zn1—O2	88.2 (4)	C8—O4—Zn1	127.2 (8)
O8—Zn1—O2	176.0 (5)	C8 ⁱ —O5—Zn2	127.1 (8)
O3—Zn1—O10	87.1 (4)	C9 ⁱⁱ —O6—Zn2	128.0 (9)
O4—Zn1—O10	178.3 (5)	C10 ⁱⁱⁱ —O7—Zn2	123.7 (7)
O9—Zn1—O10	90.6 (4)	C6—O8—Zn1	124.1 (9)
O8—Zn1—O10	88.9 (4)	C10—O9—Zn1	126.4 (6)
O2—Zn1—O10	89.1 (4)	C5—O10—Zn1	126.9 (9)
O6—Zn2—O11	95.3 (4)	C5 ^{iv} —O11—Zn2	127.8 (8)
O6—Zn2—O12	174.6 (5)	C6 ^v —O12—Zn2	124.2 (8)
O11—Zn2—O12	89.8 (4)	O10—C5—O11 ^{vi}	123.6 (11)
O6—Zn2—O1	89.2 (5)	O12 ^{vii} —C6—O8	123.0 (12)
O11—Zn2—O1	89.5 (4)	O3—C7—O1	124.4 (10)
O12—Zn2—O1	89.3 (4)	O5 ^{viii} —C8—O4	124.6 (10)
O6—Zn2—O7	92.3 (4)	O2—C9—O6 ^{ix}	127.0 (12)
O11—Zn2—O7	91.3 (4)	O9—C10—O7 ^x	123.6 (9)

O12—Zn2—O7	89.1 (4)	C2—N1—C1	113.6 (15)
O1—Zn2—O7	178.2 (6)	C3—N2—C4	114.3 (11)

Symmetry code(s): (i) $x, y+1, z$; (ii) $x, y+1, z-1$; (iii) $x+1, y+1, z-1$; (iv) $x+1, y, z-1$; (v) $x+1, y, z$; (vi) $x-1, y, z+1$; (vii) $x-1, y, z$; (viii) $x, y-1, z$; (ix) $x, y-1, z+1$; (x) $x-1, y-1, z+1$.

Table S3. Selected hydrogen-bond parameters in DMAZnD at 100 K.

$D-H\cdots A$	$D-H$ (Å)	$H\cdots A$ (Å)	$D\cdots A$ (Å)	$D-H\cdots A$ (°)
N1—H1A \cdots O7 ⁱ	0.89	1.95	2.821 (11)	167.5
N1—H1B \cdots O10 ⁱⁱ	0.89	1.93	2.819 (12)	172.0
N2—H2A \cdots O4 ⁱⁱⁱ	0.89	2.58	3.230 (17)	130.4
N2—H2A \cdots O5	0.89	1.92	2.796 (15)	169.7
N2—H2B \cdots O8	0.89	1.99	2.843 (15)	161.0

Symmetry code(s): (i) $x, y-2, z+1$; (ii) $x, y-1, z$; (iii) $x, y+1, z$.

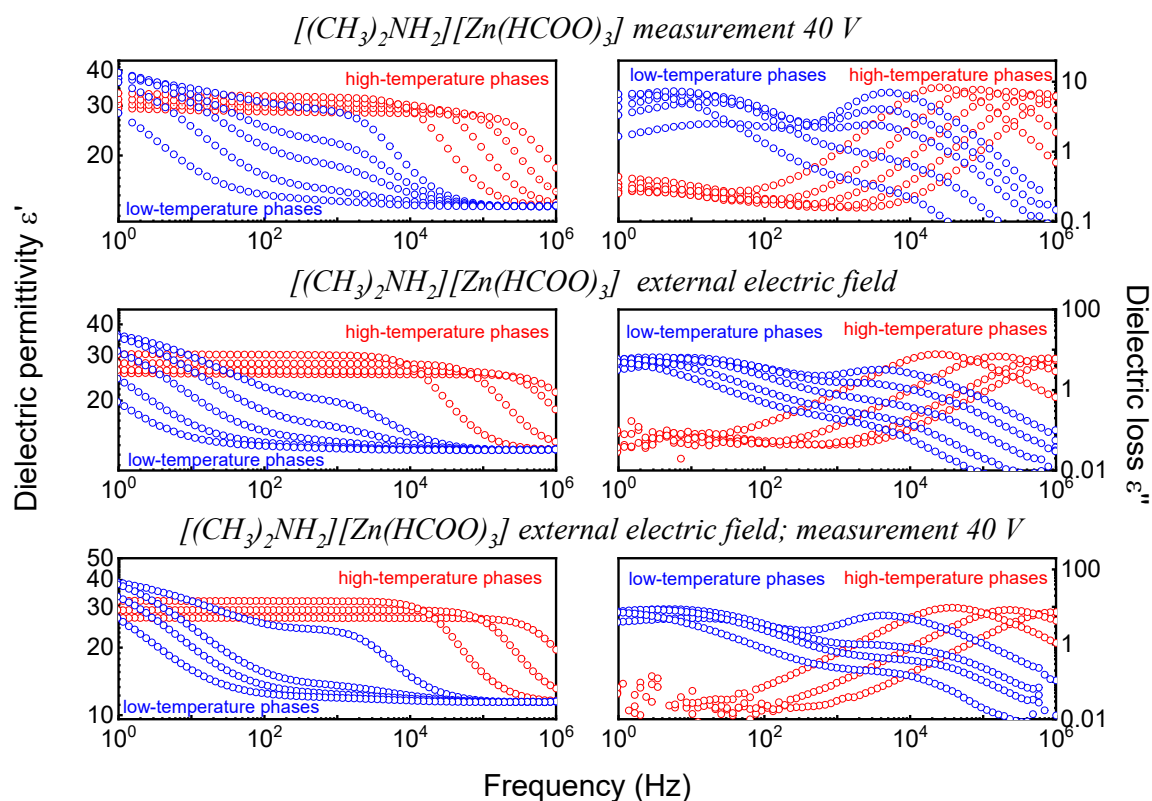


Figure S5 Frequency dependence of imaginary part of dielectric permittivity and dielectric loss. In all the investigated samples characteristic dipolar relaxation peak shifts to higher frequencies with increasing temperature

Table S4. Structure data of all possible experimental and DFT optimized phases of DMAZn

Number	Lattice parameters, experimental (Å and °)		Symmetry group, experimental	T (K)	Lattice parameters, simulated (Å)		Symmetry group, simulated	k-points	ΔE (kJ/mol/ per 2 Zn)	Alignment of DMA ⁺
1.	$a = 8.7481$ $b = 8.7600$ $c = 8.7568$	$\alpha = 55.69$ $\beta = 55.67$ $\gamma = 55.76$	$P\bar{1}$ (2)	100	$a = 8.7262$ $b = 8.8993$ $c = 8.72830$	$\alpha = 55.68$ $\beta = 55.92$ $\gamma = 55.77$	$P\bar{1}$ (2)	3x3x3	4.05	3 equivalent positions for each (excluding hydrogen atoms)
2.	$a = 8.1765$ $b = 8.1765$ $c = 22.1350$	$\alpha = 90$ $\beta = 90$ $\gamma = 120$	$R\bar{3}c$ (167)	100	$a = 8.2012$ $b = 8.2089$ $c = 22.4146$	$\alpha = 90.98$ $\beta = 88.04$ $\gamma = 119.58$	$P\bar{1}$ (1)	3x3x1	0.00	3 equivalent positions for each (including hydrogen atoms)
3.	$a = 11.8870$ $b = 8.1749$ $c = 8.8360$	$\alpha = 90$ $\beta = 95.42$ $\gamma = 90$	$C2/c$ (15)	100	$a = 11.8128$ $b = 8.3122$ $c = 8.9044$	$\alpha = 90$ $\beta = 95.49$ $\gamma = 90$	$C2/c$ (15)	3x3x3	3.96	3 equivalent positions for each (no H atoms)
4.	$a = 8.1565$ $b = 8.1572$ $c = 8.6820$	$\alpha = 63.29$ $\beta = 63.24$ $\gamma = 60.04$	$P\bar{1}$ (2)	?	$a = 8.2040$ $b = 8.2939$ $c = 8.7036$	$\alpha = 62.17$ $\beta = 63.63$ $\gamma = 60.12$	$P\bar{1}$ (2)	3x3x3	3.96	2 equivalent positions
5.	$a = 8.1391$ $b = 8.1573$ $c = 8.6779$	$\alpha = 90.00$ $\beta = 116.83$ $\gamma = 119.94$	$P\bar{1}$ (1)	100	$a = 8.2077$ $b = 8.655$ $c = 8.6797$	$\alpha = 89.97$ $\beta = 116.25$ $\gamma = 129.21$	$P\bar{1}$ (1)	3x3x3	0.10	1 non-parallel
6	-	-	Cc (9)	-	$a = 14.1721$ $b = 8.2599$ $c = 8.6913$	$\alpha = 90.0$ $\beta = 120.65$ $\gamma = 90.0$	Cc (9)	3x3x3	0.08	1 non-parallel

Table S5. Relative energy and rotation angles before and after structural optimization.

Structure number	Relative energy (kJ/mol/ per 2 Zn)	Rotation angle before optimization (°)	Rotation angle after optimization (°)
0	0	0	0
1 \equiv 0	0	45	0
2	9.29	90	101.15
3	3.84	135	119.51
4	9.39	180	221.76
5	0.03	225	239.43
6 \equiv 5	0.03	270	239.43
7 \equiv 0	0	315	360 \equiv 0
8 \equiv 0	0	360 \equiv 0	360 \equiv 0

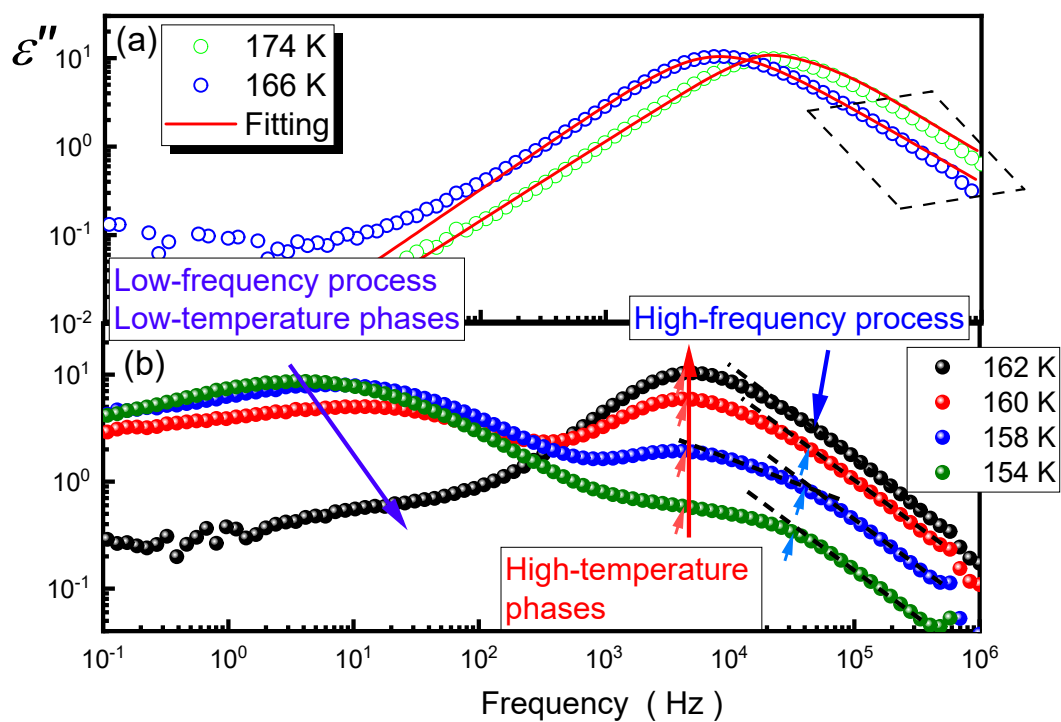


Figure S6 (a) Fits of the dielectric loss using one Havriliak-Negami functions for DMAZn_E, the high-frequency part of the relaxation peak indicate broadened. (b) The transition's region.

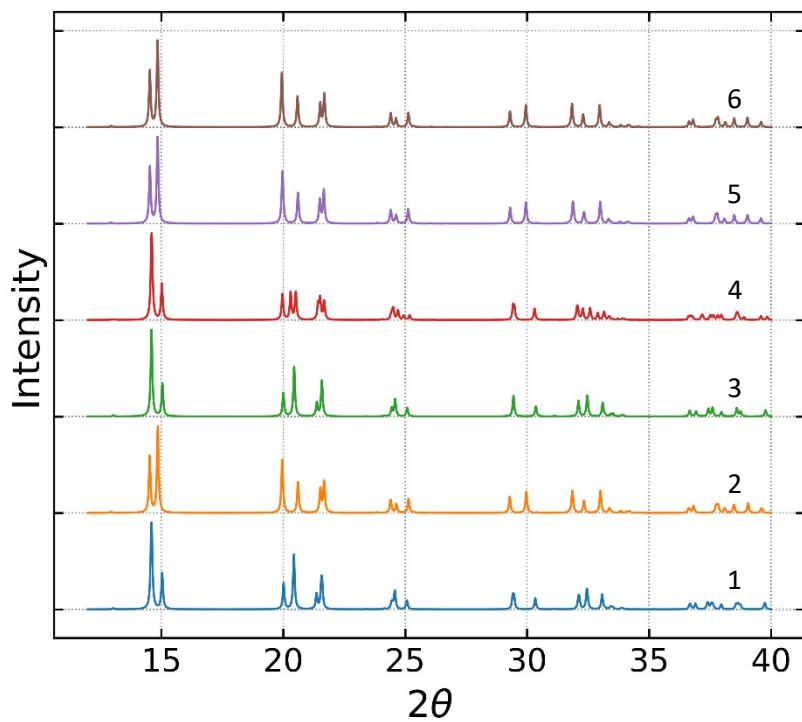


Figure S7 Calculated PXRD diffractograms for DFT-generated structures, numbers correspond to Table 1. of the main manuscript.

- 1 P. Peksa, J. Trzmiel, K. Fedoruk, A. Gagor, M. Šimenas, A. Ciupa, S. Pawlus, J. Banys, M. Mączka and A. Sieradzki, *J. Phys. Chem. C*, 2019, **123**, 23594–23603.
- 2 P. Peksa, J. Trzmiel, M. Ptak, A. Ciupa-Litwa and A. Sieradzki, *Materials (Basel)*., 2021, **14**, 6150.